

Investigations of Charge States in Co⁵⁷-Doped Oxides Using the Mössbauer-Effect and Delayed-Coincidence Techniques*

WERNER TRIFTSHÄUSER†

Physik Department, Technische Hochschule München, Munich, Germany
and

Department of Physics, University of North Carolina, Chapel Hill, North Carolina 27514

AND

DIETRICH SCHROEER

Department of Physics, University of North Carolina, Chapel Hill, North Carolina 27514

(Received 13 March 1969)

The time dependence of Fe⁵⁷ chemical charge states in sources of Cu₂O, MgO, and Al₂O₃ doped with Co⁵⁷ has been studied by means of the Mössbauer effect. Charge states of Fe¹⁺, Fe²⁺, Fe³⁺, and Fe⁴⁺ resulting from the *K*-capture decay of the Co⁵⁷ have been detected. Delayed-coincidence measurements showed no time dependence of the relative peak intensities of these charge states. A time-dependent narrowing of the resonance lines is observed which is not ascribable to "time filtering" alone. The isomer shifts of the different valence states are discussed in terms of 3*d*-electron shielding.

I. INTRODUCTION

THE technique of the Mössbauer effect (ME) has been used in a wide variety of solid-state experiments designed to study various electric, magnetic, chemical, and lattice-dynamic properties of atoms embedded in solids. It is particularly suitable for examining the properties of dilute impurities by introducing their radioactive parents into host lattices.

In a number of ME experiments, using Co⁵⁷, I¹²⁵, and Sm¹⁵³ embedded in different chemical compounds, multiple emission lines have been observed.¹⁻¹⁰ These emission lines are usually interpreted in terms of ionization states resulting from the preceding *K*-capture and Auger processes. The results of several coincidence experiments looking for a time dependence of these charge states have appeared previously.^{11,12} On the time scales available in these experiments, no time-

dependent effects were observed in the intensities of these multiple emission lines, which were not ascribable to the "time filtering"¹³ introduced by the coincidence technique itself.

We present here a study of the time and temperature dependence of the Fe⁵⁷ chemical charge states resulting from the *K*-capture decay of Co⁵⁷ in Cu₂O, MgO, and Al₂O₃. The results of this study support previous interpretations and extend our understanding of the origins and nature of such multiple charge states.

II. EXPERIMENTAL DETAILS

The Mössbauer spectra of oxides doped with Co⁵⁷ were studied at room temperature as a function of the delay time following the population of the 14.4-keV Mössbauer level in Fe⁵⁷. The technique of combining delayed-coincidence methods with the Mössbauer effect has been described earlier.^{11,12} A time-to-amplitude converter, coupled with four single-channel analyzers, is used in combination with a multichannel analyzer in the sampling mode to record Mössbauer spectra of γ rays emitted during selected time intervals following the population of the 14.4-keV Mössbauer level. The time intervals selected by the four single-channel analyzers are indicated in Fig. 1, which shows a typical coincidence spectrum of the 14.4-keV level of Fe⁵⁷ with the half-life of 100 nsec. The time scale for the measurements is limited through this half-life.

Additional Mössbauer spectra of sources of Co⁵⁷ in Cu₂O were recorded without time information, with the sources held at various temperatures. Standard cryostats were used to cool the sources of Cu₂O. The elevated temperatures were obtained by attaching the sources to a copper plate heated by current flowing through heating wires. The spectra were then recorded

* Work supported in part by the Bundesministerium für Wissenschaftliche Forschung, Bonn, Germany, by the University of North Carolina Materials Research Center under Contract No. SD-100 from the Advanced Research Projects Agency, by the U. S. Air Force under Grant No. AFOSR-69-1716 and by the National Research Council of Canada.

† Present address: Department of Physics, Queen's University, Kingston, Ontario, Canada.

¹ R. Ingalls and G. De Pasquali, *Phys. Letters* **15**, 262 (1965).

² G. K. Wertheim and R. H. Herber, *J. Chem. Phys.* **38**, 2106 (1963); G. K. Wertheim, W. R. Kingston, and R. H. Herber, *ibid.* **37**, 687 (1962); G. K. Wertheim and H. J. Guggenheim, *ibid.* **42**, 3873 (1965).

³ P. Hannaford, C. J. Howard, and J. W. G. Wignall, *Phys. Letters* **19**, 257 (1965).

⁴ G. K. Wertheim, *Phys. Rev.* **124**, 764 (1961).

⁵ R. Ingalls, C. Coston, G. De Pasquali, H. G. Drickamer, and J. Pinajian, *J. Chem. Phys.* **45**, 1057 (1966).

⁶ V. G. Bhide and G. K. Shenoy, *Phys. Rev.* **147**, 306 (1966).

⁷ C. E. Violet and R. Booth, *Phys. Rev.* **144**, 225 (1966).

⁸ E. Steichele, W. Henning, S. Hüfner, and P. Kienle, Conference on Applications of the Mössbauer Effects in Chemistry and Solid State Physics, Vienna, 1966, p. 223 (unpublished).

⁹ J. G. Mullen, *Phys. Rev.* **131**, 1415 (1963).

¹⁰ P. Jung and W. Triftshäuser, *Phys. Rev.* **175**, 512 (1968).

¹¹ W. Triftshäuser and P. P. Craig, *Phys. Rev. Letters* **16**, 1161 (1966).

¹² W. Triftshäuser and P. P. Craig, *Phys. Rev.* **162**, 274 (1967).

¹³ F. J. Lynch, R. E. Holland, and M. Hamermesh, *Phys. Rev.* **120**, 513 (1960).

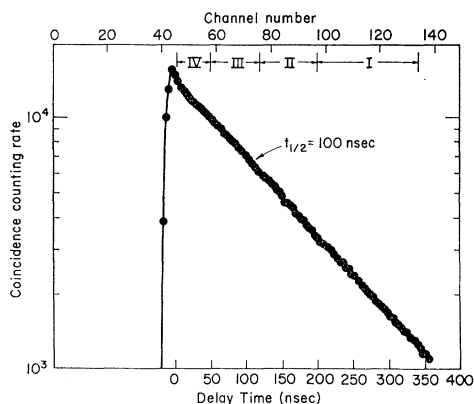


FIG. 1. A typical delayed-coincidence curve for the 14.4-keV γ ray of Fe^{57} , gated by the 122-keV γ ray preceding it. A prompt curve shows the resolution of the apparatus to be about 20 nsec. The time intervals used in the coincidence studies are indicated.

with the multichannel analyzer in the multiscaling mode.

The Co^{57} was doped into Cu_2O , MgO , and Al_2O_3 , where it should be chemically stable in the 1+, 2+, and 3+ valence state, respectively, if located at substitutional lattice sites. The MgO and Cu_2O sources were prepared by heating $\text{Mg}(\text{NO}_3)_2$ and $\text{Cu}(\text{NO}_3)_2$, to which $\text{Co}^{57}\text{Cl}_2$ has been added, in an argon atmosphere. The MgO and two Cu_2O sources [called $\text{Cu}_2\text{O}(\text{coinc})$ and $\text{Cu}_2\text{O}(1000)$ hereafter] were reduced for 4 h at 1000°C , one Cu_2O source was reduced for 4 h at 1250°C , [called $\text{Cu}_2\text{O}(1250)$ hereafter.] The resulting white (MgO) and red (Cu_2O) powders were packaged in sample holders of lucite for the

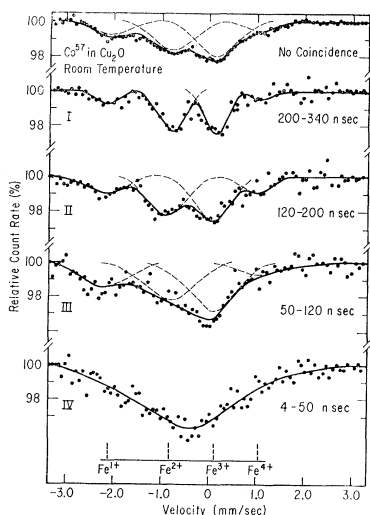


FIG. 2. Delayed-coincidence Mössbauer spectra of Co^{57} in Cu_2O . The source was prepared at 1000°C , and the spectra were taken at room temperature with a single-line absorber of $\text{K}_4\text{Fe}(\text{CN})_6 \cdot 3\text{H}_2\text{O}$. The spectrum at the top is without coincidence. The delay-time intervals used are (in nsec) (I) 200-340, (II) 120-200, (III) 50-120, and (IV) 4-50. The dashed lines are an unfolding of the spectra into time-filtered components.

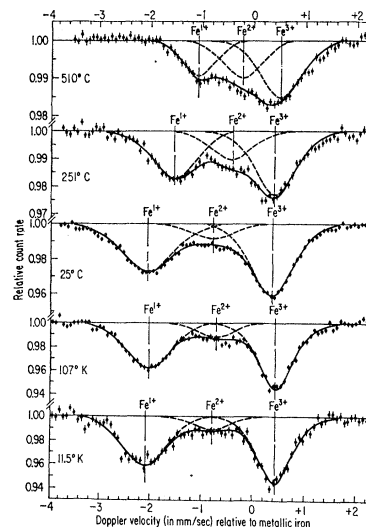


FIG. 3. Mössbauer spectra of Co^{57} in Cu_2O . The source was prepared at 1250°C . The spectra were taken against a single-line absorber of $\text{Na}_4\text{Fe}(\text{CN})_6 \cdot 10\text{H}_2\text{O}$, with the source at the temperatures indicated.

coincidence experiments, and in airtight aluminum holders in an argon atmosphere for the variable temperature measurements. Parts of these radioactive samples were investigated by x-ray goniometer techniques. No diffraction peaks not ascribable to the cubic structures of MgO and Cu_2O were observed. For the preparation of Al_2O_3 , we started with very pure Al dissolved in HCl to which trivalent Co^{57} atoms had been added (Co^{3+} was obtained by oxidizing CoCl_2 to CoCl_3). As the solution became basic, the aluminum hydroxide together with the radioactive Co^{57} was precipitated and was separated from the solution. About 50% of the Co^{57} remained in the solution. The hydroxide was converted into Al_2O_3 (white powder) by heating in an argon atmosphere at 1000°C for 4 h. The x-ray analysis demonstrated the expected crystal structure of the sample, confirming that no macroscopic distortion of the lattice had taken place.

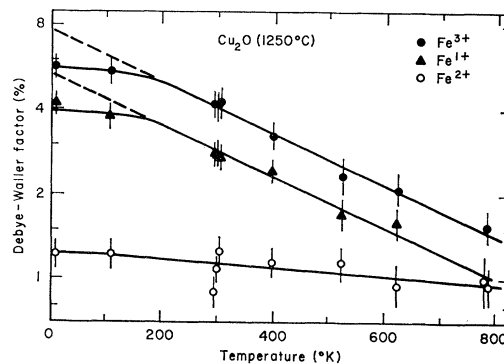


FIG. 4. Temperature dependence of the resonant fraction f of the Fe^{1+} , Fe^{2+} , and Fe^{3+} peaks in the Mössbauer spectra of Co^{57} in Cu_2O prepared at 1250°C . The straight lines are high-temperature fits for the Debye temperatures of 250 ± 30 , 600 ± 200 , and $(250 \pm 30)^\circ\text{K}$, respectively.

TABLE I. Isomer shifts (relative to iron metal), intensities, and quadrupole splittings observed for valence states observed for iron in various host lattices. Within the experimental error of about 5%, no intensity changes are observed in the various time intervals.

| Host lattice | Studies | Temp (°K) | Experimental parameter | Valence state | | | | |
|-------------------------|--------------------|-----------|---------------------------|---|------------------|------------------|------------------|--|
| | | | | Fe^{1+} | Fe^{2+} | Fe^{3+} | Fe^{4+} | |
| Cu_2O | Coincidence | 298 | Isomer shift (mm/sec) | -2.01 ± 0.05 | -0.77 ± 0.03 | $+0.14 \pm 0.03$ | $+1.14 \pm 0.03$ | |
| | | | Relative intensity | 0.17 | 0.32 | 0.42 | 0.09 | |
| | Prepared at 1000°C | 298 | Isomer shift (mm/sec) | -1.85 ± 0.10 | -0.44 ± 0.10 | $+0.32 \pm 0.10$ | $+1.14 \pm 0.20$ | |
| | | | Relative intensity | 0.19 | 0.27 | 0.47 | 0.07 | |
| | Prepared at 1250°C | 11.5 | Isomer shift (mm/sec) | -2.13 | -0.75 | +0.38 | | |
| | | | f factor | 4.2% | 1.22% | 5.7% | | |
| | | | 298 | Isomer shift (mm/sec) (meas) ^a | -2.00 | -0.64 | +0.41 | |
| | | | | Isomer shift (mm/sec) (extrap) ^a | -2.00 ± 0.10 | -0.64 ± 0.10 | $+0.57 \pm 0.10$ | |
| | | | 524 | f factor | 2.8% | 1.09% | 4.2% | |
| | | | | Isomer shift (mm/sec) | -1.54 | -0.37 | +0.40 | |
| | | | 783 | f factor | 1.71% | 1.15% | 2.3% | |
| | | | | Isomer shift (mm/sec) | -1.12 | -0.22 | +0.51 | |
| | | | f factor | 0.93% | 0.99% | 1.55% | | |
| | | | Debye temperature (°K) | 250 ± 30 | 600 ± 200 | 250 ± 30 | | |
| MgO | Coincidence | 298 | Isomer shift (mm/sec) | | -1.25 ± 0.03 | -0.41 ± 0.03 | | |
| Al_2O_3 | Coincidence | 298 | Relative intensity | | 0.48 | 0.52 | | |
| | | | Isomer shift (mm/sec) | | -1.10 ± 0.03 | -0.37 ± 0.03 | $+0.60 \pm 0.03$ | |
| | | | Relative intensity | | 0.30 | 0.47 | 0.23 | |
| | | | $\frac{1}{2}eqQ$ (mm/sec) | | 1.09 | 0.54 | 0.44 | |

^a Isomer shift (meas) is the experimentally determined isomer shift at room temperature; isomer shift (extrap) is the isomer shift extrapolated from the 11.5°K value by correcting for the second-order Doppler shift.

III. EXPERIMENTAL RESULTS

A. Co^{57} in Cu_2O

The delayed-coincidence spectra of a Co^{57} -in- Cu_2O source prepared at 1000°C [labeled $\text{Cu}_2\text{O}(\text{coinc})$] are shown in Fig. 2. A single-line absorber of $\text{K}_4\text{Fe}(\text{CN})_6 \cdot 3\text{H}_2\text{O}$ was used. The spectrum at the top was taken without coincidence and represents a time-averaged spectrum, which looks rather smeared. Through the effect of time filtering,^{13,14} we obtained in the spectra I and II several well-resolved peaks of different intensity. From their isomer shifts these were interpreted as being due to iron in the 1+, 2+, 3+, and 4+ chemical valence states. With the isomer shifts thus determined, the spectrum without coincidence and the spectra III and IV were decomposed. The broadening through time effects was taken into account by taking the line shapes from analogous spectra of a source of Co^{57} in Cu versus the same single-line absorber. The isomer shifts (relative to iron metal) and the relative intensities of these resonances are shown in Table I.

Figure 3 shows the temperature dependence of the Mössbauer spectrum of the Cu_2O source prepared at 1250°C. A single-line absorber of $\text{Na}_4\text{Fe}(\text{CN})_6 \cdot 10\text{H}_2\text{O}$ was used. The relative intensities and isomer shifts (relative to iron metal) of the resulting Fe^{1+} , Fe^{2+} , and Fe^{3+} resonances are recorded in Table I, and are shown, respectively, in Figs. 4 and 5. The observed effects in the resonance spectra were temperature reversible. The intensities in Fig. 4 are fitted to the high-temperature approximation¹⁵ for the Debye-

Waller factor f :

$$\ln f = C + 6E_r T / k\Theta_D^2, \quad (1)$$

where C is a constant, E_r is the recoil energy, T is the temperature, and Θ_D is the Debye temperature. We find Debye temperatures of $250 \pm 30^\circ\text{K}$, $600 \pm 200^\circ\text{K}$, and $250 \pm 30^\circ\text{K}$, respectively, for the 1+, 2+, and 3+ resonances.

Figure 6 shows the temperature dependence of the Mössbauer spectrum of the $\text{Cu}_2\text{O}(1000)$ source. A single-line absorber of $\text{Na}_4\text{Fe}(\text{CN})_6 \cdot 10\text{H}_2\text{O}$ was used. Again the temperature effects were reversible. The

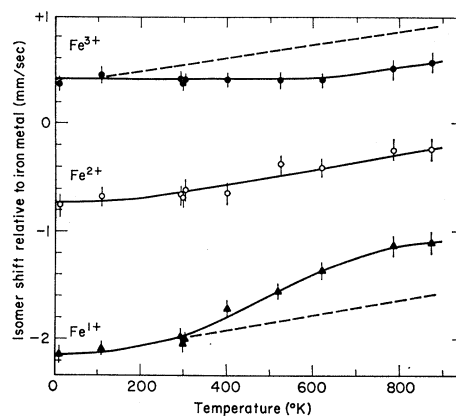


FIG. 5. Temperature dependence of the resonant velocities of the Fe^{1+} , Fe^{2+} , and Fe^{3+} peaks in the Mössbauer spectra of Co^{57} in Cu_2O prepared at 1250°C. The dashed lines are fits of the data to the second-order Doppler-shift equation for the Debye temperatures of 250, 600, and 250°K, respectively.

¹⁴ C. S. Wu, Y. K. Lee, N. Benczer-Koller, and P. C. Simms, *Phys. Rev. Letters* **5**, 432 (1960).

¹⁵ R. H. Herber and G. K. Wertheim, in *The Mössbauer Effect*,

edited by D. M. J. Compton and A. Schoen (Wiley-Interscience, Inc., New York, 1962), p. 105.

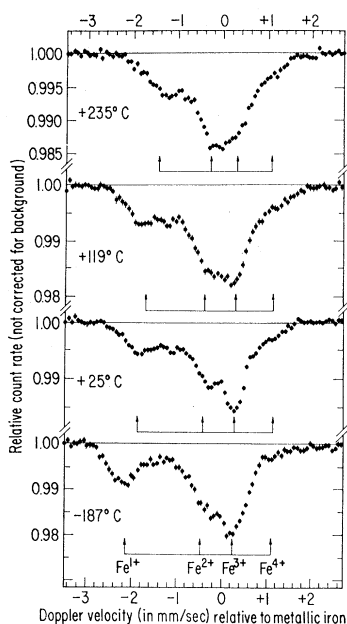


FIG. 6. Mössbauer spectra of Co^{57} in Cu_2O . The source was prepared at 1000°C . The spectra were taken against a single-line absorber of $\text{Na}_4\text{Fe}(\text{CN})_6 \cdot 10\text{H}_2\text{O}$, with the source at the temperatures indicated.

absolute intensities of the Fe^{1+} , Fe^{2+} , Fe^{3+} , and Fe^{4+} resonance peaks are shown in Fig. 7 as a function of the temperature. The room-temperature values of the absolute intensities and the isomer shift (relative to iron metal) are shown in Table I.

B. Co^{57} in MgO

Figure 8 shows the time-dependent Mössbauer spectra of Co^{57} in MgO , against a single-line absorber of $\text{K}_4\text{Fe}(\text{CN})_6 \cdot 3\text{H}_2\text{O}$, taken at room temperature. Only the two valence states Fe^{2+} and Fe^{3+} were observed. Table I presents the isomer shift (relative to iron metal) and the relative peak intensities of these resonance peaks. Again no time dependence of the peak

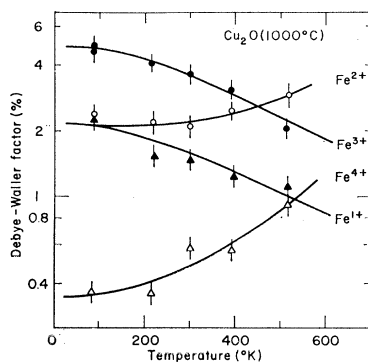


FIG. 7. Temperature dependence of the resonant fraction f of the Fe^{1+} , Fe^{2+} , Fe^{3+} , and Fe^{4+} peaks in the Mössbauer spectra of Co^{57} in Cu_2O prepared at 1000°C .

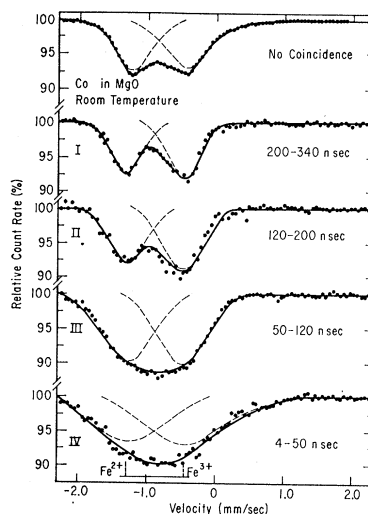


FIG. 8. Delayed-coincidence Mössbauer spectra of Co^{57} in MgO . The spectra were taken at room temperature with a single-line absorber of $\text{K}_4\text{Fe}(\text{CN})_6 \cdot 3\text{H}_2\text{O}$. The spectrum at the top is taken without coincidence. The delay-time intervals used are (in nsec) (I) 200-340, (II) 120-200, (III) 50-120, and (IV) 4-50. The dashed lines are an unfolding of the spectra into time-filtered components.

intensities was observed for the various delay-time intervals.

C. Co^{57} in Al_2O_3

Figure 9 shows the results of time-dependent measurements with the source of Co^{57} in Al_2O_3 and a single-line absorber of $\text{K}_4\text{Fe}(\text{CN})_6 \cdot 3\text{H}_2\text{O}$. The three charge states Fe^{2+} , Fe^{3+} , and Fe^{4+} were observed, with no

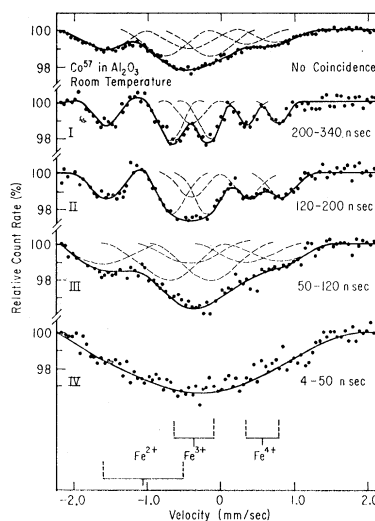


FIG. 9. Delayed-coincidence Mössbauer spectra of Co^{57} in Al_2O_3 . The spectra were taken at room temperature with a single-line absorber of $\text{K}_4\text{Fe}(\text{CN})_6 \cdot 10\text{H}_2\text{O}$. The spectrum at the top is taken without coincidence. The delay-time intervals used are (in nsec) (I) 200-340, (II) 120-200, (III) 50-120, and (IV) 4-50. The dashed lines are an unfolding of the spectra into time-filtered components.

time dependence of the relative peak intensities. The spectra taken with the delay-time intervals I (200–340 nsec) and II (120–200 nsec) clearly indicate a quadrupole splitting of each resonance peak. The isomer shifts relative to iron metal, the relative intensities, and the quadrupole splittings of these resonance peaks are shown in Table I.

IV. DISCUSSION AND CONCLUSIONS

A. Time Dependence of Spectra

The delayed-coincidence spectra of Figs. 2, 8, and 9 show the time dependence observed earlier.^{11–14} As indicated in these earlier papers,^{13,14} this broadening is due to the time filtering according to the Heisenberg uncertainty principle. However, the following question arises: The natural linewidth (2Γ) for the 14.4-keV Fe^{57} Mössbauer level is 0.19 mm/sec. For example, while the resonance lines for the $\text{Cu}_2\text{O}(\text{coinc})$ source in the time-averaged spectrum are about 1.0 mm/sec wide, the absorber linewidth (with a Co^{57} -in-Cu source) is only 0.28 mm/sec. This indicates that the larger part of the resonance line broadening is not due to absorber thickness. If this broadening is due to time-independent source inhomogeneities, then no time filtering of this broadening would be expected. Yet it is experimentally observed in our spectra. The linewidth for the $\text{Cu}_2\text{O}(\text{coinc})$ -source spectrum taken in the delay interval I (200–340 nsec) is about 0.6 mm/sec wide. This narrowing of 0.4 mm/sec is far beyond that expected from any conceivable reduction of the natural linewidth due to the Heisenberg uncertainty principle. For the MgO and Al_2O_3 sources, similar excessively large narrowing is observed, although the effect is not quite as pronounced. If part of the source line broadening is due to relaxation phenomena, this part could be reduced by time filtering. Relaxation phenomena, which might cause these effects, include the excitation of localized lattice vibrational modes, temporary changes in atomic force constants, higher charge states, and atomic states which produce appreciably different quadrupole splittings in the excited and equilibrium states, etc.¹⁶ Through the K -capture and the subsequent Auger processes, any or all of these phenomena may occur; from these experiments it is not possible to distinguish among the various possibilities. The observation of the time-dependent narrowing indicates that the relaxation phenomena die out on a time scale comparable to the nuclear lifetime of the resonant level. The occurrence of such relaxation phenomena is intimately connected with the microscopic stoichiometry around the decaying atom, and with the strength of the bonding and hence the Debye temperature.¹⁰

Except for this time-dependent narrowing, the Mössbauer spectra for each of the sources studied are

identical for the various delay times. Within the experimental error of about 5%, the relative intensities of the various iron charge states resulting from the K -capture decay of the Co^{57} atoms doped into these oxides are time-independent during the time interval of 5–340 nsec following the population of the 14.4-keV Mössbauer level. These results are in agreement with earlier measurements^{11,12} on other compounds. They support the conclusion that, especially in oxides containing cation vacancies or excess oxygen, chemical valence states higher and/or lower than the chemical equilibrium state can be stabilized. They are apparently established in less than 5×10^{-9} sec, and they can exist longer than 3×10^{-7} sec (and are possibly stable), as indicated by their constant intensity within the lower and upper limits of our time resolution.

B. Co^{57} in Cu_2O

The x-ray analyses of the various sources in each case indicate the appropriate macroscopic crystal structure. However, the ME samples the microscopic surroundings of the emitting Mössbauer nucleus, and these are apparently quite different depending on source preparation. The emission spectra of the oxides doped with Co^{57} each exhibit several resonance peaks. The four resonances for the $\text{Cu}_2\text{O}(\text{coinc})$ and $\text{Cu}_2\text{O}(1000)$ sources (both prepared at 1000°C) are interpreted as being due to Fe^{4+} , Fe^{2+} , Fe^{3+} , and Fe^{4+} , as indicated in Figs. 2 and 6. The three resonance peaks in the spectrum of $\text{Cu}_2\text{O}(1250)$ are interpreted analogously as Fe^{4+} , Fe^{2+} , and Fe^{3+} , as indicated in Fig. 3.

These charge-state assignments are made on the basis of the isomer shifts and their temperature dependence as well as on the basis of the valences expected from the chemical preparation. The Fe^{2+} and Fe^{3+} isomer shifts at room temperature agree with those usually observed for such states and indicate a 4s-electron admixture of $x=22\%$, as determined from the Walker-Wertheim-Jaccarino diagram¹⁷ of Fig. 10. In Figs. 2, 6, and 7 the Fe^{4+} and Fe^{4+} resonances would be expected to fall to the left of the Fe^{2+} resonance and to the right of the Fe^{3+} resonance, respectively, in agreement with our interpretation. There does, however, exist the possibility that the observed peaks are in reality halves of quadrupole splittings of the Fe^{2+} and Fe^{3+} resonance, respectively, with the other halves hidden, respectively, under the Fe^{3+} or Fe^{2+} resonance. This possibility is rejected for the 3+ state because the experimental splitting would have to be about 2 mm/sec wide to fit Figs. 2 and 6, whereas the quadrupole splittings of Fe^{3+} ions are typically of the order of 0.5 mm/sec.^{18,19} For the Fe^{2+} resonance, this quadrupole-

¹⁷ L. R. Walker, G. K. Wertheim, and V. Jaccarino, *Phys. Rev. Letters* **6**, 98 (1961).

¹⁸ W. Kerler and W. Neuwirth, *Z. Physik* **167**, 176 (1962).

¹⁶ J. G. Dash and R. H. Nussbaum, *Phys. Rev. Letters* **16**, 567 (1966).

¹⁹ H. Wegener, *Der Mössbauer Effekt und seine Anwendung in Physik und Chemie* (Bibliographisches Institut Mannheim, Mannheim, Germany, 1966), p. 144.

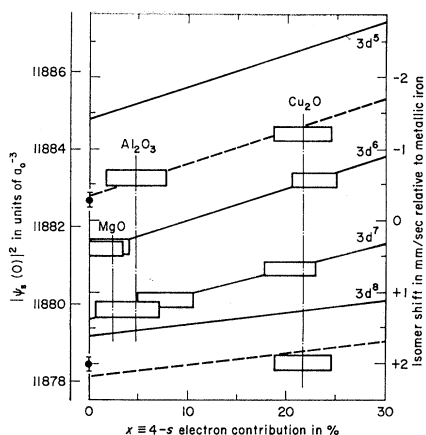


FIG. 10. A Walker-Wertheim-Jaccarino plot of the Fe^{57} isomer shift versus $4s$ -electron density for various $3d$ -electron configurations (Refs. 17 and 32). The isomer shifts are relative to Fe metal (note the reversal of the scale as compared to Table I to allow comparison with absorber experiments). The present data are plotted with the dashed vertical lines indicating equal covalent bonding. The dashed inclined lines show the experimental behavior for the Fe^{1+} and Fe^{4+} ions as opposed to the theoretically calculated solid lines.

splitting possibility is rejected because the expected temperature dependence of an Fe^{2+} quadrupole splitting is not observed. Typical quadrupole splittings at low temperatures for divalent iron ions are about 3 mm/sec,¹⁸ in agreement with the value calculated from the equation¹⁹

$$\Delta\nu(\text{Fe}^{2+}, T \rightarrow 0) = \mp(2/7)(1-R)(e^2Q/E)\langle r^{-3} \rangle_{3d} = 3.1 \text{ mm/sec}, \quad (2)$$

with the values of $R=0.42$ for the atomic Sternheimer factor, $\langle r^{-3} \rangle = 35 \times 10^{24} \text{ cm}^3$, $E=14.4 \text{ keV}$, and $Q=0.18 \times 10^{-24} \text{ cm}^2$. To fit the data of Figs. 2, 3, and 6, the splitting of the Fe^{2+} state at 11.5°K would have to be about 2.2 mm/sec, small compared to the typical values. As the temperature increases, the spacing between the Fe^{1+} and Fe^{3+} peaks does decrease, just as a quadrupole-split Fe^{2+} doublet would; and this decrease is reversible. However, the decrease is approximately linear with temperature between 128 and 350°C, and then appears to level off at yet higher temperatures. In contrast, the quadrupole splitting of an Fe^{2+} ion collapses much more abruptly as the temperature increases, since exponential Boltzmann factors control the population of the relevant crystal field states.¹⁹

The temperature dependences of the isomer shifts of the Fe^{1+} and Fe^{3+} peaks are not explainable solely on the basis of the second-order Doppler shift. Figure 5 shows the isomer-shift data for the $\text{Cu}_2\text{O}(1250)$ source fitted at low temperatures with Debye temperatures of 250, 600, and 250°K for the Fe^{1+} , Fe^{2+} , and Fe^{3+} resonances, respectively, using the formula for the second-order Doppler shift of Pound and Rebka.²⁰ At high tempera-

tures the shifts of the Fe^{1+} and Fe^{3+} peaks are too large to be so fitted. We suggest that these temperature-dependent isomer shifts are due to changes in the nature of the chemical bonding with temperature. There are two possibilities. (a) The bonding may become more covalent with increasing temperature. The shift of about 0.5 mm/sec over and above the second-order Doppler shift for the Fe^{1+} resonance peak would correspond to an increase in $4s$ -electron density of about 30% (see Fig. 10). (b) These shifts could be due to changes in the number of $3d$ electrons. For the Fe^{1+} peak a decrease of about 0.5 $3d$ electrons would be sufficient to explain the shift. The first possibility seems unlikely, as it would require the nature of the chemical bond of the Fe^{1+} and Fe^{3+} state to be very much different from that of the other Fe states in the Cu_2O . The second possibility appears to be not unreasonable. At elevated temperatures, the mobility of electrons (and hence the electron shell overlap) increases, so that it is quite possible for one of the $3d$ electrons of the Fe^{1+} ion to be partially (increasing with temperature) shared with some neighboring atoms around a vacancy. For the Fe^{3+} ion a similar mechanism might operate to increase the effective shielding of the $3d$ electrons. Vorobev and Karkhanin²¹ have stated that in Cu_2O samples associated groups of lattice defects (Cu^+ vacancies) exist which dissociate into single vacancies during illumination with light and increasing temperature, so that the effective number of vacancies is increased. The Fe^{1+} and Fe^{3+} peaks in the $\text{Cu}_2\text{O}(1000)$ source are shifted in the direction observed at the higher temperatures for the $\text{Cu}_2\text{O}(1250)$ source. This supports the argument that these shifts are due to defects, since the $\text{Cu}_2\text{O}(1000)$ source is expected to contain more defects.

For all of these reasons, we assume that the two outer peaks in the $\text{Cu}_2\text{O}(1000)$ spectrum at low temperatures correspond to Fe^{1+} and Fe^{4+} ions with the same $4s$ -electron admixture as those of the Fe^{2+} and Fe^{3+} ions. The values used in the discussion are extrapolated to room temperatures by correcting for the second-order Doppler shift.

The relative intensities of the various resonance peaks support our multiple-valence-states interpretation. In the Cu_2O samples either one monovalent copper atom may be replaced substitutionally by a monovalent radioactive Co^{57} atom, or else two copper atoms may be replaced by one divalent cobalt atom, which may or may not be on a regular lattice site. Higher valence should not exist *a priori*, i.e., before the electron-capture decay. The replacement of two Cu^{1+} atoms by one Co^{2+} atom produces vacancies in the neighborhood of the decaying atom. These holes, together with the lower oxygen density in Cu_2O , might be favorable for stabilizing higher-energy charge states, as has been suggested

²⁰ R. V. Pound and G. A. Rebka, Jr., Phys. Rev. Letters 4, 274 (1960).

²¹ Yu. V. Vorobev and Yu. I. Karkhanin, Fiz. Tverd. Tela 7, 1865 (1965) [English transl.: Soviet Phys.—Solid State 7, 1500 (1965)], and references cited therein.

earlier for CoO doped with Co^{57} .¹² The occurrence of the Fe^1 resonance peak is therefore not surprising, and the low Debye temperature $\Theta_D(1+) = 250^\circ\text{K}$ of this resonance indicates that it is substitutional, as expected. The high Debye temperature $\Theta_D(2+) = 600^\circ\text{K}$ of the Fe^{2+} resonance indicates that this is an interstitial ion. The Fe^{3+} resonance with its low Debye temperature of $\Theta_D(3+) = 250^\circ\text{K}$ appears to be substitutional, and must be stabilized by neighboring defects. The origin of the Fe^{4+} resonance is not clear, but it must involve stabilization by some defects.

The preparation temperature of 1250°C for the $\text{Cu}_2\text{O}(1250)$ source is high enough to liquify the source. We would expect this treatment to increase the probability of Co^{57} entering the lattice substitutionally, and to reduce the number of defects present in the lattice. This expectation is consistent with the observation that the substitutional Fe^{1+} peak is enhanced in the $\text{Cu}_2\text{O}(1250)$ source, while the interstitial and defect stabilized Fe^{2+} and Fe^{4+} resonance peaks are suppressed.

Figure 7 shows the temperature dependence of the intensities of the four resonances in the Mössbauer spectra of the $\text{Cu}_2\text{O}(1000)$ source. This figure indicates a reversible interchange between the various valence states, similar to the observed in CoO.^{12,22} In particular, the Fe^{2+} and Fe^{4+} peaks increase with temperature. This indicates that perhaps part of the reason for the indicated high Debye temperature of the Fe^{2+} state in the $\text{Cu}_2\text{O}(1250)$ source might be some conversion of one of the other valence state into the divalent state. However, the isomer shifts, as a function of the temperature for the Fe^{2+} state in the same source, do fit the $\Theta_D = 600^\circ\text{K}$ second-order Doppler-shift curve. In the case of CoO, two interpretations were offered for the reversible interconversion between Fe^{2+} and Fe^{3+} valence states. Ok and Mullen²² suggested that there exist two different physical phases of CoO, one with bulk properties showing only the Fe^{2+} resonance, and one with a half-vacant lattice showing only the Fe^{3+} resonance. The interchange between the di- and trivalent iron is then due to interchanges between these two phases. Triftshäuser and Craig,¹² on the other hand, interpreted the interconversion as being due to the increasing mobility of the vacancies. This results at higher temperature in an increased stabilization of the Fe^{3+} charge state. In this case of Co^{57} in Cu_2O , more than two ionic states are involved in the interconversion. Since it seems unlikely that there are four physically different phases of Cu_2O , all showing the same x-ray patterns, the charge-stabilization theory appears to be the more satisfactory one, insofar as it can explain both the CoO and the Cu_2O data.

C. Co^{57} in MgO

In the case of Co^{57} in MgO, the two valence states Fe^{2+} and Fe^{3+} were observed (Fig. 8) in contrast to

²² H. N. Ok and J. G. Mullen, *Phys. Rev.* **168**, 550 (1968).

measurements published previously where Fe^{1+} appeared additionally.²³ Three valence states were also observed for Co^{57} in CaO.²⁴ The lattice structure of CaO and MgO is the same (fcc), and therefore the Co^{57} should enter the MgO exclusively as a divalent substitutional atom. However, in MgO both di- and trivalent iron atoms can be stabilized.^{25,26}

D. Co^{57} in Al_2O_3

The emission spectra of the Al_2O_3 doped with Co^{57} show three quadrupole-split resonances, which we interpret as due to Fe^{2+} , Fe^{3+} , and Fe^{4+} ions in noncubic surroundings, as indicated in Fig. 9. Most of the preparation of Co^{57} -doped Al_2O_3 in the past has been carried out by diffusing divalent cobalt atoms into the Al_2O_3 lattice. Then it is found^{25,27} that they occur in the lattice only in the divalent state, but both in substitutional and interstitial lattice sites. Because of charge compensation, these two sites should be occupied in the ratio of one interstitial to two substitutional atoms, so that three divalent Co atoms replace two trivalent Al atoms.²⁸ On the other hand, it is known that iron enters Al_2O_3 only as a trivalent substitutional atom.²⁵ For the preparation of our sample we started with trivalent cobalt atoms, and therefore the probability of obtaining substitutional Co^{3+} atoms should be enhanced. In agreement therefore with Wertheim *et al.*,²⁵ we interpret the Fe^{2+} resonance as arising from interstitial divalent cobalt atoms and the Fe^{3+} resonance as arising from substitutional divalent and trivalent cobalt atoms. We cannot determine whether the Fe^{4+} states are produced from interstitial or substitutional cobalt atoms, but one would expect them to originate from trivalent substitutional cobalt atoms. The observed quadrupole splittings in Fig. 8 are consistent with our valence-state assignments. The $3d$ -electron shell of the Fe^{3+} ion is exactly half-filled, so that the electric field gradient (EFG) at the site of the nucleus is due only to that produced by the crystalline electric field. It consequently leads to small quadrupole splittings on the order of 0.5 mm/sec,¹⁹ in agreement with our observation of 0.54 mm/sec. The Fe^{2+} ion, on the other hand, will display a temperature-dependent quadrupole splitting, as discussed earlier.¹⁹ This is in agreement with the larger quadrupole splitting of 1.09 mm/sec observed for the Fe^{2+} resonance. The Fe^{4+} ion has a hole in the half-filled $3d$ -electron shell. This can also lead to a temperature-dependent modification of the EFG at the site of the nucleus, with the modification oppositely directed

²³ R. B. Frankel and N. A. Blum, *Bull. Am. Phys. Soc.* **12**, 24 (1967).

²⁴ J. Chappert, R. B. Frankel, and N. A. Blum, *Bull. Am. Phys. Soc.* **12**, 352 (1967).

²⁵ Reference 15, p. 130.

²⁶ E. R. Feher, *Phys. Rev.* **136**, A145 (1964).

²⁷ G. K. Wertheim and J. P. Remeika, *Phys. Letters* **10**, 14 (1964).

²⁸ G. M. Zverev and A. M. Prokhorov, *Zh. Eksperim. i Teor. Fiz.* **12**, 41 (1961) [English transl.: *Soviet Phys.—JETP* **12**, 41 (1961)].

to that in the case of the Fe^{2+} ion. The slightly smaller quadrupole splitting for the Fe^{4+} resonance of 0.44 mm/sec, compared to that of the Fe^{3+} resonance, is consistent with this picture. Exact descriptions of these effects would depend on the positions of the ions inside the lattice.

E. Isomer-Shift Recalibration

The experiment with the Cu_2O sources is the first time that four valence states have been observed simultaneously. This result is well suited to examine the dependence of the isomer shift on the number of $3d$ electrons, i.e., the direct influence on the $3d$ -electron shielding. The isomer shift measured in a ME experiment is

$$\delta = \frac{4}{5}\pi Z e^2 R^2 (\delta R/R) S' [|\psi_s(0)|_A^2 - |\psi_s(0)|_S^2], \quad (3)$$

where δR is the change in the nuclear radius from the excited state to the ground state, $|\psi_s(0)|_A^2$ and $|\psi_s(0)|_S^2$ are, respectively, the total s -electron densities at the nucleus for the absorber and for the source, and S' is a relativistic correction factor. Watson²⁹ carried out Hartree-Fock calculations of the s -electron density at the nucleus $|\psi_s^{3d^n}(0)|^2$ for different $3d$ configurations of iron. The results show that especially the $3s$ -electron density changes significantly if the number of $3d$ electrons varies, while the change in $|\psi_{1s}(0)|^2$ and $|\psi_{2s}(0)|^2$ is substantially smaller. Hartree-Fock calculations do not account for the $4s$ -electron density. However, the Fermi-Segrè-Goudsmit³⁰ formula allows a rather accurate estimate of this density if the term values of the $3d^n 4s^1$ configurations are known.³¹

Walker *et al.*¹⁷ established an isomer-shift calibration between the calculated s -electron densities and the measured isomer shifts of various iron compounds, identifying the isomer shifts in the most ionic Fe^{2+} and Fe^{3+} compounds, respectively, with the calculated densities for the $3d^6$ and $3d^5$ configurations. We have extended the $4s$ -density calculation in the $3d^4 4s^1$ configuration, and for the other configurations we used the values given by Wegener.³² Figure 10 presents the calculated curves together with the measured isomer shifts. The intersections with the $3d^n 4s^x$ curves are marked with bars which include the uncertainties in the measured data. A small covalent bonding is found which differs slightly among the various oxides. Because of its particular chemical structure, Cu_2O should contain a larger fraction of covalent bonding than the other oxides.³³

²⁹ R. E. Watson, MIT Technical Report No. 12, 1959 (unpublished).

³⁰ E. Fermi and E. Segrè, *Z. Physik* **82**, 729 (1933); S. Goudsmit, *Phys. Rev.* **43**, 636 (1933).

³¹ H. H. Landolt and R. Börnstein, *Zahlenwerte und Funktionen* (Springer-Verlag, Berlin, 1950), Vol. 1.

³² Reference 19, p. 199.

³³ L. Pauling, *The Nature of the Chemical Bond* (Cornell University Press, Ithaca, N. Y., 1960).

The $2+$ and $3+$ states measured in the Cu_2O sample fit well on the calculated electron-density curves, respectively, for a $3d^6 4s^0$ ²² and a $3d^5 4s^0$ ²² configuration. We will assume that the $1+$ and the $4+$ valence states at *low temperatures* also contain about 22% covalent bonding, i.e., that they also have a 22% admixture of $4s$ electrons. This assumption of similar bonding mechanisms for the various charge states is reasonable, particularly in the light of charge compensation. The experimental isomer-shift values for Fe^{1+} and Fe^{2+} , however, differ considerably from the calculated values corresponding to 22% $4s$ electrons. A similar behavior is found in the Al_2O_3 sample, where the $2+$ and $3+$ states show reasonable agreement with the calculated data (x about 5%), while the additional isomer shift for the $4+$ state is only about half of the calculated value. In MgO , where only $2+$ and $3+$ valence states are observed, the agreement is good, and almost pure ionic bonding is indicated. The isomer shifts measured earlier¹¹ for Fe^{2+} and Fe^{3+} in CoO fit also very well on the curves with x about 3%. To test these calculations of the s -electron density further, we have plotted two additional isomer-shift data, namely, those for Fe^{1+} in NaCl as measured by Mullen⁹ and for Fe^{4+} in cobalt ammonium sulphate as measured by Ingalls *et al.*¹ These compounds are assumed to have almost pure ionic bonding, and they appear therefore at $x=0$ in Fig. 10. These data are consistent with our experimental isomer shifts, as indicated by the dashed lines drawn connecting them, and inconsistent with the theoretical predictions, as indicated by the solid lines. The disagreement is not so much with the $4s$ -electron density calculations—the slopes of the dashed and solid lines are the same—but rather with the shielding effects of the $3d$ -electron.

This discrepancy between theory and experiment is presumably due to the fact that these calculations were carried out using free-ion wave functions. The large measured isomer shifts for the Fe^{1+} states indicate a very low electronic charge density at the nucleus. The polarization of s electrons is one effect which decreases the electron density, and in order to obtain sufficient polarization to explain the measured isomer shift, a $3d^7$ configuration has to be ascribed to the Fe^{1+} atom.^{9,34} As far as we know, no polarization effects have been taken into account for the electron density calculation, so that the disagreement of the measurements with the calculations is not too surprising.

The polarization effect means that, under certain circumstances, as in our experiments, for example, in the configurations $3d^4$ to $3d^7$, every $3d$ electron shields a more or less constant part of the $3s$ electrons. Further investigations should be carried out to explore these discrepancies.

³⁴ W. Hayes, *J. Appl. Phys. Suppl.* **33**, 329 (1962).